Carbon and other light element contents in the Earth's core based on first-principles molecular dynamics

Yigang Zhang[a] and Qing-Zhu Yin[b,1]

[a]Key Laboratory of the Earth's Deep Interior, Institute of Geology and Geophysics, Chinese Academy of Sciences, Beijing 100029, China; and [b]Department of Geology, University of California, Davis, CA 95616

Edited by Mark H. Thiemens, University of California at San Diego, La Jolla, CA, and approved October 19, 2012 (received for review March 5, 2012)

Carbon (C) is one of the candidate light elements proposed to account for the density deficit of the Earth's core. In addition, C significantly affects siderophile and chalcophile element partitioning between metal and silicate and thus the distribution of these elements in the Earth's core and mantle. Derivation of the accretion and core–mantle segregation history of the Earth requires, therefore, an accurate knowledge of the C abundance in the Earth's core. Previous estimates of the C content of the core differ by a factor of ~20 due to differences in assumptions and methods, and because the metal–silicate partition coefficient of C was previously unknown. Here we use two-phase first-principles molecular dynamics to derive this partition coefficient of C between liquid iron and silicate melt. We calculate a value of 9 ± 3 at 3,200 K and 40 GPa. Using this partition coefficient and the most recent estimates of bulk Earth or mantle C contents, we infer that the Earth's core contains 0.1–0.7 wt% of C. Carbon thus plays a moderate role in the density deficit of the core and in the distribution of siderophile and chalcophile elements during core–mantle segregation processes. The partition coefficients of nitrogen (N), hydrogen, helium, phosphorus, magnesium, oxygen, and silicon are also inferred and found to be in close agreement with experiments and other geochemical constraints. Contents of these elements in the core derived from applying these partition coefficients match those derived by using the cosmochemical volatility curve and geochemical mass balance arguments. N is an exception, indicating its retention in a mantle phase instead of in the core.

The high solubility of C in liquid iron (1, 2) and the existence of graphite and cohenite $(Fe,Ni)_3C$ in iron meteorites (3) suggest that C could account for the density deficit of the Earth's core (4–6). Carbon content also greatly influences siderophile and chalcophile element partitioning between metal and silicate, and hence their distribution in the Earth's core and mantle (7, 8). In particular, its influence on Pb partitioning would affect the inference of the age of the Earth (9). Therefore, it is critically important to constrain the C content of the Earth's core.

There are several ways to infer the C content of the core. The first method is a solubility and phase diagram study in the Fe–C system, which generally gives a high C content in the Earth's core, on the order of 2–4 wt% (1). The implicit assumption is that C is supersaturated during the Earth's accretion process, and so this study will generally give the maximum C content of the core. The second method involves density and bulk modulus measurements of solid Fe_3C and Fe_7C_3 under the inner core pressures and comparison with the seismic data of the inner core. This kind of study results in a C content of 1–1.5 wt% (10, 11) and assumes that C is the only light element in the inner core, thus giving only an upper limit for the C content in the inner core. Application of the density and bulk modulus measurements of solid and liquid Fe_3C to the outer core exclude C as a major alloying element in the Earth's outer core (12, 13). The third method is based on carbonaceous chondrite composition, the element volatility curve of the bulk Earth, and the mass balance between primitive mantle and core. This method gives the smallest C content of the core: 0.2 wt% (14).

Thus, the C content of the core has proven to be difficult to constrain, and current estimates differ by a factor of ~20. Some limits on the geochemical role of C in the core-forming process can be provided by P, which becomes lithophile during C saturation (7). Because P is depleted rather than enriched in the mantle, core formation probably did not occur at C saturation (7). Thus, we contend that the starting bulk composition of the Earth may have contained a lower C content than some of the experiments outlined above indicated.

Carbon is thought to have entered the core through core–mantle segregation processes in the early history of the Earth during the magma ocean stage. Inferring the amount of C involved thus requires determining the partition coefficient of C between liquid iron and silicate melt experimentally. However, as yet no such data exist, as pointed out by Dasgupta and Walker (15). Many partitioning experiments for siderophile elements use C as a sample encapsulating material, thus greatly affecting the behavior of these elements.

In the present study, we use the two-phase first-principles molecular dynamics (FPMD) method (16) to determine the partition coefficient of C and a few other light elements between liquid iron and silicate melt. This partition coefficient can then be combined with the composition of the bulk Earth or the primitive mantle (i.e., bulk silicate Earth) to infer the C content of the Earth's core.

Results and Discussion

The starting bulk composition of the FPMD simulation (Table 1) is a simplified version of the composition of bulk Earth (14), with all of the lithophile elements added to Mg, siderophile elements to Fe, and O and Si left unchanged. The O/Si weight ratio is 1.98, which is in between the so-called O-bearing (O/Si = 2.16) and Si-bearing (O/Si = 1.84) bulk Earth composition (14). This is to keep the oxidation state of the simulation in between the O-bearing and Si-bearing bulk Earth compositional models of ref 14. The temperature and pressure of the simulation are fixed at 3200 K and 40 GPa, which are chosen based on the single-stage magma ocean depth inferred from siderophile element distribution (17, 18). In general, the Earth's accretion history is expected to be more complicated (19), but the single-stage magma ocean model can be viewed as an effective model reflected by the siderophile element distribution in the mantle (20).

At the beginning of the simulation, atoms are placed randomly into the simulation box. After 30,000 steps, the atoms are segregated into two phases, a liquid iron phase and a silicate melt phase. Fig. 1 shows a snapshot of atom configurations with segregated phases and the constructed alpha shape for calculating the number of atoms enclosed in the Fe cluster. A total of 32,000 such snapshots are used to calculate the average compositions of the liquid iron and silicate melt phases (Table 1). Based on these

Author contributions: Y.Z. and Q.-Z.Y. designed research; Y.Z. and Q.-Z.Y. performed research; Y.Z. contributed new reagents/analytic tools; Y.Z. and Q.-Z.Y. analyzed data; and Y.Z. and Q.-Z.Y. wrote the paper.

The authors declare no conflict of interest.

This article is a PNAS Direct Submission.

[1]To whom correspondence should be addressed. E-mail: qyin@ucdavis.edu.

Table 1. Starting composition and simulation results

Phases	Unit*	O	Mg	Fe	Si	C
Starting composition of run M47						
Bulk	no.a	125	51	44	36	4
Bulk	wt%	29.6	18.4	36.4	15.0	0.7
Compositions after simulation of run M47						
Liquid iron	no.a	1.2 (2)	0.013 (6)	43.998 (1)	1.5 (2)	3.4 (2)
Liquid iron	wt%	0.8 (1)	0.012 (6)	96.0 (3)	1.6 (2)	1.60 (9)
Silicate melt	no.a	123.8 (2)	50.987 (6)	0.002 (1)	34.5 (2)	0.6 (2)
Silicate melt	wt%	47.2 (8)	29.5 (2)	0.003 (1)	23.1 (2)	0.17 (6)

Data in parentheses are the errors on the last digit estimated using the block average method (41).
*no.a denotes number of atoms.

compositions, the partition coefficient of C between liquid iron and silicate melt is found to be 9 ± 3.

To derive the C content of the core, we need the C content of the Earth's mantle (C^M) or the bulk Earth (C^E). Previous inferences of mantle C content span a very large range from 20 to 300 ppm (21). The large range is caused in part by the lack of knowledge of the relative size of the volatile depleted and enriched mantle source regions. Marty (22) points out that derivation of volatile element abundance in the bulk mantle does not have to depend on the reservoir sizes and estimates mantle C content using the abundance of ^{40}Ar, N/^{40}Ar, C/N, and C/^{4}He ratios (22). Marty (22) gives a C content of 526 ± 206 ppm for the bulk Earth, which is the sum of atmospheric and mantle inventories and normalized to the total mass of the Earth. The value when normalized to the mass of the mantle is 780 ± 306 ppm. By using our partition coefficient and assuming that the core and the mantle C contents were connected through a single-stage magma ocean process at 40 GPa and 3200 K, the core would contain (780 ± 306 ppm) × 9 ≈ 0.7 ± 0.3 wt% C. Using the C content of the Earth's mantle provided by ref. 14, the Earth's core would contain 0.1% of C.

This amount of C implies that it plays a moderate role in the core density deficit. The impact of C content on siderophile and chalcophile element distribution in the Earth's core and mantle will need to be critically evaluated. Carbon is known to increase siderophility of V, Cr, Mn (8), W, and Mo (7), but it appears to have no effect on Ni and Co (23), Os, and Ir (24). Ge, which belongs to the same group as C and Pb, shows a strong increase of its partition coefficient in the absence of C (7), which corroborates the findings of Wood and Halliday (9).

Additional FPMD calculations are made for systems containing the same numbers of O, Mg, Fe, and Si as run M47, but with elements H, He, P, or N replacing C (Table 2). The partition coefficient of He is found to be ~9×10^{-3}, in close agreement with the most recent laser-heated diamond-anvil cell experiments (25), but disagrees with earlier data based on piston and cubic anvil press experiments (26), which is 10^{-4} when extrapolated to 10 GPa. For an exchange reaction between two phases, the reaction constant, which is the ratio of the activities of the products to those of the reactants, does not change at a fixed temperature and pressure. However, the partition coefficient, which is the ratio of concentrations, does vary at the same temperature and pressure due to the variation of the activity coefficient with concentration. Thus, care should be taken when comparing and using partition coefficients that have been obtained at very different concentration ranges. For example, the two experiments mentioned above (25, 26) were performed at very different He concentrations, which might explain the different partition coefficients.

We obtain a partition coefficient for N of 1.8 ± 0.2, which is in general agreement with recent experimental data, giving a value of ~3 at 1.5 GPa (27) and 5–15 at 4–15 GPa (28). We also

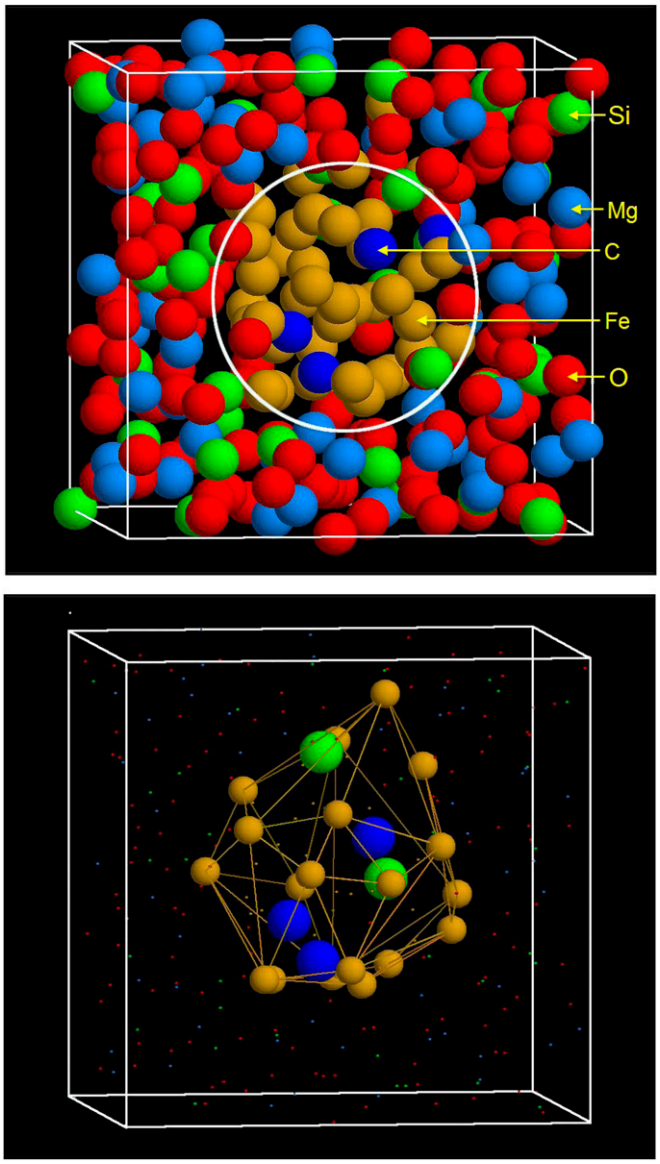

Fig. 1. (*Upper*) Snapshot of atomic configuration in the simulation cell after the center of mass of the Fe cluster is moved to the center of the simulation cell and all of the atoms are moved accordingly by using the periodic conditions of the simulation cell. The encircled area marks the liquid metal phase domain and the surrounding area is the silicate melt domain. (*Lower*) The constructed alpha shape of the Fe cluster showing Fe atoms on the surface of the alpha shape and the Si and C atoms enclosed in the alpha shape.

obtain a partition coefficient for H of ~0.7 ± 0.1, suggesting H was weakly lithophile during the magma ocean period. This contradicts the strong siderophile behavior inferred in a previous study (29). However, the H partition coefficient between iron and ringwoodite is 26 at 1273 K and 16.6–20.9 GPa (30). Using $D_{Fe/melt} = D_{Fe/ringwoodite} \times D_{ringwoodite/melt}$ and $D_{ringwoodite/melt}$ of ~0.03 (31, 32), the partition coefficient of H between iron and silicate melt would be 26 × 0.03 ≈ 0.8. This is again in close agreement with our data. The similarity of our results to the results of previous experimental studies demonstrates that two-phase FPMD is a viable method for determining element partition coefficients between liquid iron and silicate melt.

The Earth's mantle contains roughly 6% Fe, mainly as FeO; however, our calculated mantle composition contains a negligible amount of Fe (Tables 1 and 2). This discrepancy is an artifact

Table 2. Simulation results for systems containing H, C, P, He, and N

Runs	O	Mg	Fe	Si	LE	LE-ID	Partition coef*
M46	1.2 (2)	0.09 (4)	95.8 (3)	2.8 (2)	0.046 (7)	H	0.7 (1)
	47.4 (2)	29.8 (1)	0.06 (4)	22.6 (1)	0.069 (4)		
M47	0.8 (1)	0.012 (6)	96.0 (3)	1.6 (2)	1.60 (9)	C	9 (3)
	47.2 (8)	29.5 (2)	0.003 (1)	23.1 (2)	0.17 (6)		
M48	1.2 (1)	0.13 (4)	92.7 (4)	2.5 (2)	3.5 (1)	P	4.5 (5)
	47.0 (1)	29.5 (1)	0.2 (2)	22.5 (1)	0.77 (8)		
M51	1.1 (1)	0.07 (3)	96.4 (3)	2.4 (2)	0.004 (2)	He	0.009 (6)
	47.2 (1)	29.6 (1)	0.06 (2)	22.7 (1)	0.381 (1)		
M52	1.0 (1)	0.06 (3)	95.8 (3)	2.0 (2)	1.15 (8)	N	1.8 (2)
	47.0 (1)	29.5 (1)	0.03 (2)	22.8 (1)	0.63 (5)		
Partition coef†	0.022 (7)	0.002 (2)	N/A	0.10 (2)			

All of the compositions listed are in weight percent. For each run, the upper row is the liquid iron composition and the lower row is the silicate melt composition. Numbers in parentheses are the uncertainties on the last digit calculated using the block average method (41). Note that the Fe content of the silicate melt is underestimated. LE, light element; LE-ID, identity of the light element. Partition coefficient is defined as a ratio of concentration between liquid iron and silicate melt (wt% in metal/wt% in silicate).

*Partition coefficients listed in the last column are the partition coefficients of the light elements for H, C, P, He, and N.

†Partition coefficients listed in the bottom row are the partition coefficients of O, Mg, and Si.

of the small system size used in our calculation. When the system is small, Fe atoms on the surface of the Fe cluster occupy a large proportion of the total number of Fe atoms. These Fe atoms should be divided between the interfacing phases of silicate mantle and the metallic core. Our low Fe concentrations result from attributing all of the Fe atoms on the cluster surface as the core Fe concentration. The calculated concentration of Fe of the core depends on how the Fe atoms on the cluster surface are divided. Imagine a perfect cube cluster shape where the Fe atoms occupy the surface. Depending on where the Fe atoms are located, the distribution between the two boundary phases will be different. Those atoms on the flat surface would be equally distributed between the silicate mantle and the metallic core, those on the rim will have one-fourth inside the core and three-fourths in the silicate phase, and each of those atoms on the eight corners of the cube will have only one-eighth inside the core and seven-eighths shared with the silicate mantle. In reality, the alpha shape constructed for the Fe cluster (Fig. 1 *Lower*) is of an irregular shape. In such a case, there is no clear-cut way to divide the Fe atoms on the surface between the metallic core and silicate mantle, because the surfaces are not smooth. In a system of an infinitely large size, treating all of the Fe atoms on the cluster surface as core Fe atoms would have negligible effects on the mantle composition of Fe, because the cluster surface Fe would represent a very small fraction of the total Fe in either the silicate mantle or in metallic core phases. Unfortunately, computation of such a large system is unrealistically expensive and time-consuming with the presently available computing power. Thus, the artifact of very low Fe in the silicate mantle is unavoidable for a small system size until a realistic criterion is developed for dividing cluster-surface Fe between metallic core and silicate mantle. It is therefore meaningless to use the concentration of Fe calculated for the silicate mantle and the metallic core (Tables 1 and 2) to compute the oxygen fugacity of the system.

To critically evaluate further whether the artifact of very low Fe in the silicate mantle would affect other light elements partitioning into the core (the main focus of the present work), we have performed additional FPMD simulations to calculate the solubility of Si in liquid iron coexisting with silicate melt at the pressures and temperatures of magma oceans relevant to the Earth's core formation (Table 3) and compared the results with the recent state-of-the-art, laser-heated diamond-anvil cell and multianvil press experiments (33, 34). The reason for choosing Si as an example instead of C is simply because no experimental data exist for C solubility in liquid iron coexisting with silicate melt and at carbon undersaturated condition. This highlights the technical difficulties to obtain experimental data for C, which makes our theoretical approach particularly valuable to fill in the niche in our knowledge gap.

We fitted the Si solubility as a function of P (pressure) and T (temperature) using the following relationship:

$$\mathrm{Si(wt\%)} = \mathrm{A} + \mathrm{B} \times T + \mathrm{C} \times P + \mathrm{D} \times P \times T$$

for the two bulk Earth compositional models of (14), respectively, where the coefficients A, B, C, and D are inverted using the data in Table 3. This step is necessary to compare the Si solubility data obtained under the exact pressures and temperatures

Table 3. FPMD results of Si solubility in liquid iron at various pressures and temperatures

Runs	T (K)	P (GPa)	Si (wt%)	1σ
"Si-bearing" Earth composition				
M9	3,116	38.8	2.43	0.27
M16	3,116	59.2	3.30	0.28
M19	3,800	40.0	5.00	0.34
M20	3,800	59.6	5.12	0.30
M21	3,500	39.9	4.43	0.32
M22	4,100	40.6	6.13	0.41
M23	3,800	22.3	5.51	0.33
M32	3,800	79.0	4.97	0.27
M33	3,800	97.9	4.59	0.26
M56	4,200	120.4	5.14	0.28
M61	2,500	19.7	2.26	0.26
"O-bearing" Earth composition				
M24	3,116	39.8	1.92	0.29
M25	3,800	38.7	3.60	0.36
M26	3,116	55.9	1.41	0.18
M27	3,800	58.5	3.16	0.18
M57	3,800	77.0	3.11	0.29
M58	4,000	97.7	3.42	0.29
M59	4,200	118.9	4.22	0.30
M60	2,500	19.6	0.78	0.18

"Si-bearing" Earth composition (14) contains 29.2% O, 18.4% Mg, 36.5% Fe, and 15.8% Si. "O-bearing" Earth composition (14) contains 30.4% O, 18.5% Mg, 36.8% Fe, and 14.3% Si (all in weight percent).

with diamond-anvil and multianvil experiments (33, 34). As can be seen in Fig. 2, the agreements between the experiments (33, 34) and our calculations are within ~1% over a large pressure and temperature range. If the molar ratio of total cations to oxygen of the bulk systems is considered as a proxy for the oxidation state of the systems, the agreements between the experiments (33, 34) and our FPMD calculation are even better. Deviation of this ratio from unity is primarily governed by the multiple oxidation states of major element Fe (0, +2, +3). The remarkable agreement of our FPMD calculations with the experiments (Fig. 2) clearly demonstrates that the lower Fe content in silicate melt in our FPMD runs does not affect our calculated results of light elements in the core, the key focus of the paper. Because the experiments (33, 34) were performed at a relevant mantle oxidation state (oxygen fugacity about 2 log units below the iron–wüstite buffer), we argue that our calculated partition coefficients are applicable to the Earth's interior.

Suppose we are able to assign correctly ~6% Fe into the mantle (we only need to move ~4.8 Fe atoms from the metallic phase into the silicate phase); the result would be an increase in the concentration of light elements in the core by ~10% compared with the values reported in Table 2. This would be in closer agreement with the results of experimental studies (33, 34). Increasing the Fe content in the mantle would also increase the calculated partition coefficients by ~20%, generally within the errors of the values that we present for D in Table 2. Therefore, we did not apply any bias corrections for this effect.

The compositions of the Earth's core inferred using different methods are compared in Fig. 3. Core compositions given by McDonough (14) are inferred by combining the average composition of carbonaceous chondrites, the volatility curve, and the estimated composition of bulk silicate Earth. Our methods use newly obtained partition coefficients based on FPMD, and either the bulk Earth or primitive mantle compositions (14, 22) as input data, to estimate the light element contents in the Earth's core. As illustrated in Fig. 3, based on the partition coefficient calculated for Mg, the Earth's core contains a small amount of Mg. The core contents of Si, O, C, P, and H, inferred using theoretical

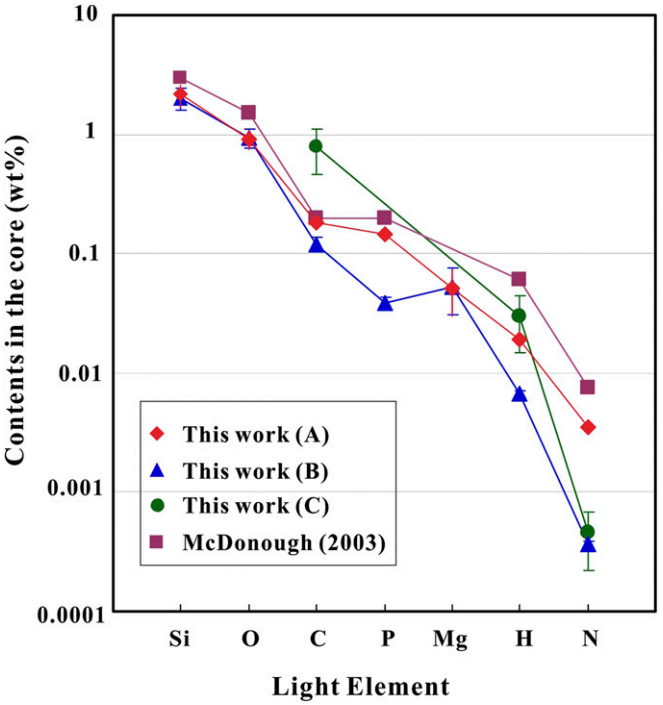

Fig. 3. Comparison of Si, O, C, P, Mg, H, and N contents of the Earth's core derived using different methods. Red diamonds [this work (A)] show an estimate of the core composition using $C^C = C^E/[f + (1 - f)/D]$, where C^C represents core composition, C^E is bulk Earth composition (14), f is mass fraction of metallic core, and D is partition coefficients from Table 2. Blue triangles [this work (B)] show the core composition derived using the definition of partition coefficient, the $C^C = D \times C^M$, where C^M is the primitive mantle composition (bulk silicate Earth) of ref. 14. Green circles [this work (C)] show the use of the most recent estimates of C, H, and N of the Earth's mantle (22) and our *ab-initio* partition coefficients to calculate the corresponding core composition using $C^C = D \times C^M$. Purple squares are the core compositions given by McDonough (14) based on volatility curve, cosmochemical constraints, and mass balance of geochemical reservoirs. With the exception of N, core compositions of light elements agree within an order of magnitude or better between different approaches.

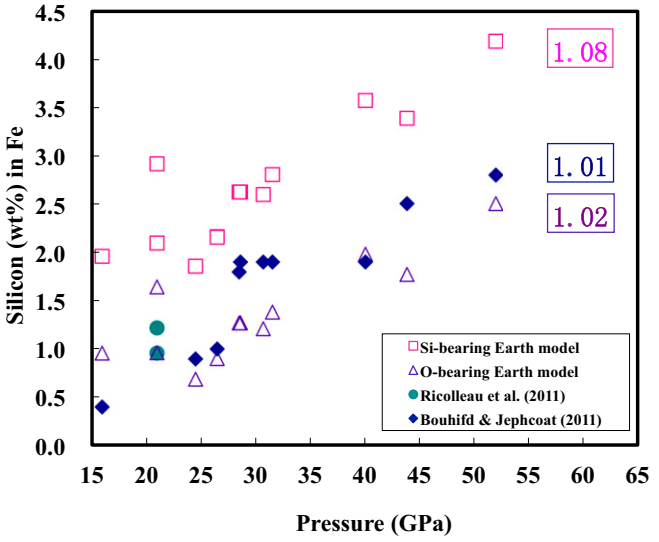

Fig. 2. Comparison of Si solubility in liquid iron obtained by FPMD with experimental data (33, 34). Temperatures and pressures are exactly as in the experiments (33, 34). The rectangles with numbers inside are the molar ratio of total cations to oxygen of the bulk system (metallic phase + silicate phase), controlling the oxidation state of the bulk system. The 1.08 is for the Si-bearing and 1.02 is for the O-bearing Earth models of Table 3, and 1.01 is for experimental data (33).

and empirical methods, are in general agreement to the first order. The higher C contents in the Earth's core, represented by the solid green circle in Fig. 3, results from the high C content of the mantle (ref. 22) used in the calculation $C^C = D \times C^M$ (Fig. 3). In fact, the partition coefficient resulted from the volatility curve method is ~10 (ref. 14) and the same as ours within error. For N, the core N content in McDonough (14) using the volatility curve is comparable to our calculated value (red diamond in Fig. 3) within a factor of 2. However, using the current mantle values of N from either McDonough (14) or Marty (22) would give a lower value of N in the Earth's core by an order of magnitude (blue triangle and green circle in Fig. 3). This suggests that either our calculated partition coefficient is too low by a factor of 10 or we do have a "missing nitrogen" problem in the mantle, as has been suggested as an alternative to N in the core (22). The latter requires the assumption that the volatile elemental ratio of the Earth is chondritic, as indicated by the distribution of many volatile elements (22). Otherwise, if the inferred partition coefficient of 1.8 ± 0.2 and mantle inventory of N are both correct, the Earth would be depleted in N as a whole.

Conclusions

The partition coefficient of C between liquid iron and silicate melt is determined to be 9 ± 3 based on FPMD. Assuming that C is distributed between the Earth's core and mantle through

magma ocean processes, the core is inferred to contain between 0.1–0.7 wt% C. Carbon thus plays a moderate role in the core density deficit and in the chalcophile and siderophile element distribution during core–mantle segregation processes. We further demonstrate that two-phase FPMD is a viable method by showing that it can provide partition coefficients that are in close agreement with experimental data and geochemical observations. Light element contents of the Earth's core inferred by applying the partition coefficients agree with those derived from using the cosmochemical volatility curve of elements and geochemical mass balance arguments. Nitrogen deviates the most from this general agreement, suggesting a potential missing N problem for the Earth's mantle.

Methods

The method used in the present study is similar to that in Zhang and Guo (ref. 16) and is described only briefly here. Calculations are performed by using the *ab-initio* total-energy and molecular-dynamics program VASP (35). The projector-augmented wave potentials (36, 37) are used together with the generalized gradient approximation of the exchange-correlation potential (PBE, ref. 38). The plane-wave basis set cutoff is 400 eV. The accuracy for electronic self-consistent iteration is 10^{-4} eV. The Brillouin zone sampling is performed only at the gamma point. The Fermi–Dirac smearing is used to consider the temperature effect.

Molecular dynamics simulations are performed in the NVT ensemble with a time step of 1 fs. Our "experimental charges" are composed of 260 atoms. The starting configuration is a random distribution of atoms in the simulation cell; 20,000 to ~30,000 steps are used for the two phases (liquid iron and silicate melt) to segregate and for the system to reach equilibrium. During this period, total energy of the system first decreases and then fluctuates around a plateau value. Then the system is simulated for another 30,000–50,000 steps to accumulate atom positions for composition calculations.

At each FPMD step, the number of atoms enclosed in the Fe phase is obtained by first constructing a polyhedron for the Fe cluster and then judging whether an atom is enclosed in the polyhedron by using concepts and methods in computational geometry (39). Basically, three steps are needed. First, the center of mass of the Fe cluster is calculated and moved to the center of the simulation cell. All atoms are moved accordingly by using the periodic boundary conditions of the simulation cell. This is the preparatory step for using the computational geometry. Second, an alpha shape is constructed for the Fe cluster by using the program "hull" (40), which employs the randomized incremental algorithm. Third, whether an atom is inside the constructed polyhedron in the second step is determined by using the program "inhedron" (39), which employs the random ray crossing algorithm.

The atoms in the simulation box exchange between silicate-melt and liquid-iron phases, and their numbers in the phases vary during FPMD simulations. This can be viewed as a dynamic equilibrium process. The numbers of atoms in the Fe phase at each FPMD step are summed and averaged over the whole accumulation period of the simulation to calculate the composition of the Fe phase. Composition of the silicate melt can be directly derived as the bulk composition of the whole system is known.

ACKNOWLEDGMENTS. This work was supported by Chinese Academy of Sciences Grant KZCX2-YW-Q08-1 and National Science Foundation of China Grant 41020134003. Grant Z201003 (to Q.-Z.Y.) from the State Key Laboratory of Lithospheric Evolution, Institute of Geology and Geophysics, Chinese Academy of Sciences in part enabled this work.

1. Wood BJ (1993) Carbon in the core. *Earth Planet Sci Lett* 117(3–4):593–607.
2. Nakajima Y, Takahashi E, Suzuki T, Funakoshi K-I (2009) "Carbon in the core" revisited. *Phys Earth Planet Inter* 174(1–4):202–211.
3. Buchwald VF (1975) *Handbook of Iron Meteorites, Their History, Distribution, Composition, and Structure* (Univ of California Press, Berkeley).
4. Birch F (1952) Elasticity and constitution of the Earth's interior. *J Geophys Res* 57: 227–286.
5. Stevenson DJ (1981) Models of the Earth's core. *Science* 214(4521):611–619.
6. Poirier J-P (1994) Light elements in the earth's outer core: A critical review. *Phys Earth Planet Inter* 85(3–4):319–337.
7. Jana D, Walker D (1997) The impact of carbon on element distribution during core formation. *Geochim Cosmochim Acta* 61(13):2759–2763.
8. Chabot NL, Agee CB (2003) Core formation in the Earth and Moon: New experimental constraints from V, Cr, and Mn. *Geochim Cosmochim Acta* 67(11):2077–2091.
9. Wood BJ, Halliday AN (2010) The lead isotopic age of the Earth can be explained by core formation alone. *Nature* 465(7299):767–770.
10. Fiquet G, Badro J, Gregoryanz E, Fei Y, Occelli F (2009) Sound velocity in iron carbide (Fe_3C) at high pressure: Implications for the carbon content of the Earth's inner core. *Phys Earth Planet Inter* 172(1–2):125–129.
11. Mookherjee M, et al. (2011) High-pressure behavior of iron carbide (Fe_7C_3) at inner core conditions. *J Geophys Res* 116:B04201, 10.1029/2010JB007819.
12. Sata N, et al. (2010) Compression of FeSi, Fe_3C, $Fe_{0.95}O$, and FeS under the core pressures and implication for light element in the Earth's core. *J Geophys Res* 115: B09204, 10.1029/2009JB006975.
13. Terasaki H, et al. (2010) Density measurement of Fe_3C liquid using X-ray absorption image up to 10 GPa and effect of light elements on compressibility of liquid iron. *J Geophys Res* 115:B06207, 10.1029/2009JB006905.
14. McDonough WF (2003) Compositional model for the Earth's core. *The Mantle and Core, Vol. 2. Treatise on Geochemistry*, ed. Carlson RW (Elsevier-Pergamon, Oxford), pp. 547–568.
15. Dasgupta R, Walker D (2008) Carbon solubility in core melts in a shallow magma ocean environment and distribution of carbon between the Earth's core and the mantle. *Geochim Cosmochim Acta* 72(18):4627–4641.
16. Zhang YG, Guo GJ (2009) Partitioning of Si and O between liquid iron and silicate melt: A two-phase ab-initio molecular dynamics study. *Geophys Res Lett* 36:L18305, 10.1029/2009GL039751.
17. Corgne A, Siebert J, Badro J (2009) Oxygen as a light element: A solution to single-stage core formation. *Earth Planet Sci Lett* 288(1–2):108–114.
18. Wade J, Wood BJ (2005) Core formation and the oxidation state of the Earth. *Earth Planet Sci Lett* 236(1–2):78–95.
19. Rubie DC, et al. (2011) Heterogeneous accretion, composition and core-mantle differentiation of the Earth. *Earth Planet Sci Lett* 301(1–2):31–42.
20. Rudge JF, Kleine T, Bourdon B (2010) Broad bounds on Earth's accretion and core formation constrained by geochemical models. *Nat Geosci* 3:439–443.
21. Hirschmann MM, Dasgupta R (2009) The H/C ratios of Earth's near-surface and deep reservoirs, and consequences for deep Earth volatile cycles. *Chem Geol* 262(1–2):4–16.
22. Marty B (2012) The origins and concentrations of water, carbon, nitrogen and noble gases on Earth. *Earth Planet Sci Lett* 313–314:56–66.
23. Chabot NL, Draper DS, Agee CB (2005) Conditions of core formation in the Earth: Constraints from Nickel and Cobalt partitioning. *Geochim Cosmochim Acta* 69(8): 2141–2151.
24. Brenan JM, McDonough WM (2009) Core formation and metal–silicate fractionation of osmium and iridium from gold. *Nat Geosci* 2:798–801.
25. Jephcoat AP, Bouhifd MA, Porcelli D (2008) Partitioning experiments in the laser-heated diamond anvil cell: Volatile content in the Earth's core. *Philos Transact A Math Phys Eng Sci* 366(1883):4295–4314.
26. Matsuda J, et al. (1993) Noble gas partitioning between metal and silicate under high pressures. *Science* 259(5096):788–790.
27. Kadik AA, et al. (2011) Influence of oxygen fugacity on the solubility of nitrogen, carbon, and hydrogen in FeO-Na_2O-SiO_2-Al_2O_3 melts in equilibrium with metallic iron at 1.5 GPa and 1400 °C. *Geochem Int* 49(5):429–438.
28. Roskosz M, Bouhifd MA, Jephcoat AP, Marty B, Mysen BO (2012) Nitrogen solubility in molten metal and silicate at high pressure and temperature: A first experimental approach. *Proceedings of the 43rd Lunar Planetary Science Conference* (Lunar and Planetary Institute, Houston, TX), 1497.
29. Okuchi T (1997) Hydrogen partitioning into molten iron at high pressure: implications for Earth's core. *Science* 278(5344):1781–1784.
30. Shibazaki Y, Ohtani E, Terasaki H, Suzuki A, Funakoshi KI (2009) Hydrogen partitioning between iron and ringwoodite: Implications for water transport into the Martian core. *Earth Planet Sci Lett* 287(3–4):463–470.
31. Kawamoto T, Hervig RL, Holloway JR (1996) Experimental evidence for a hydrous transition zone in the early Earth's mantle. *Earth Planet Sci Lett* 142(3–4):587–592.
32. Ohtani E, Mizobata H, Yurimoto H (2000) Stability of dense hydrous magnesium silicate phases in the systems Mg_2SiO_4-H_2O and $MgSiO_3$-H_2O at pressures upto 27 GPa. *Phys Chem Miner* 27(8):533–544.
33. Bouhifd MA, Jephcoat AP (2011) Convergence of Ni and Co metal-silicate partition coefficients in the deep magma-ocean and coupled silicon-oxygen solubility in iron melts at high pressures. *Earth Planet Sci Lett* 307(3–4):341–348.
34. Ricolleau A, Fei Y, Corgne A, Siebert J, Badro J (2011) Oxygen and silicon contents of Earth's core from high pressure metal-silicate partitioning experiments. *Earth Planet Sci Lett* 310(3–4):409–421.
35. Kresse G, Furthmüller J (1996) Efficient iterative schemes for ab initio total-energy calculations using a plane-wave basis set. *Phys Rev B Condens Matter* 54(16): 11169–11186.
36. Blöchl PE (1994) Projector augmented-wave method. *Phys Rev B Condens Matter* 50 (24):17953–17979.
37. Kresse G, Joubert D (1999) From ultrasoft pseudopotentials to the projector augmented-wave method. *Phys Rev B* 59(3):1758–1775.
38. Perdew JP, Burke K, Ernzerhof M (1996) Generalized gradient approximation made simple. *Phys Rev Lett* 77(18):3865–3868.
39. O'Rourke J (1998) *Computational Geometry in C* (Cambridge Univ Press, Cambridge, UK), 2nd Ed.
40. Clarkson KL, Mehlhorn K, Seidel R (1993) Four results on randomized incremental constructions. *Comp Geom* 3(4):185–212.
41. Allen MP, Tildesley DJ (1987) *Computer Simulation of Liquids* (Clarendon, Oxford).